Cooperation between Lateral Ligand Mobility and Accessibility for Receptor Recognition in Selectin-Induced Cell Rolling[†,#]

Udo Bakowsky,[‡] Gabriele Schumacher,[§] Christian Gege,[∥] Richard R. Schmidt,[∥] Ulrich Rothe,[⊥] and Gerd Bendas*[,§]

Department of Membrane Cell Biology, University of Groningen, 9700 AD Groningen, The Netherlands, Department of Pharmacy, Martin-Luther-University Halle, Wolfgang-Langenbeck-Strasse 4, D 06120 Halle, Germany, Department of Chemistry, University Konstanz, Box M725, D 78457 Konstanz, Germany, and Institute of Physiological Chemistry, Martin-Luther-University Halle, Hollystrasse 1, D 06097 Halle, Germany

Received September 5, 2001; Revised Manuscript Received January 7, 2002

ABSTRACT: Selectin-induced leukocyte rolling along the endothelial surface is an essential step in the immune response. Several in vitro studies showed that this cell rolling is a highly regulated adhesion phenomenon, controlled by the kinetics and forces of selectin−ligand interactions. In the flow chamber study presented here, we focused on the requirements on the ligand structure in this context. A series of neoglycolipids bearing the binding epitope Sialyl Lewis X was synthesized and used as artificial ligands. These lipids differed in their spacer structures between headgroup and membrane anchor, resulting in a gradual variation in accessibility and mobility of the binding epitope when immobilized in model membranes. Consequently, analysis of cell rolling along such membranes allowed correlation of ligand structures and functionality. All model membranes containing such ligands were further characterized by film balance measurements, epifluorescence, and atomic force microscopy. Generally, the glycolipids exhibited a high tendency for lateral aggregation, but the resulting clusters were of different morphology. This was also reflected by strong differences in the rolling experiments. Our results confirm that, in addition to a sufficient headgroup accessibility, the cell rolling process is governed by two further interdependent factors: (i) the headgroup flexibility caused by the intramolecular uncoupling between the headgroup and the hydrophobic moiety due to introduction of a spacer, and (ii) the stiffness of the molecules resulting from their supramolecular arrangement in clustered assemblies. Since both factors are influenced simultaneously by the spacer modification, we present for the first time a clear correlation between structural aspects of selectin ligands and their ability to mediate cell rolling. This might help to develop a better understanding for the function of the natural selectin ligands.

The receptor-mediated recruitment of leukocytes to sites of inflammation is essential for the development of an appropriate immune response. The leukocyte adhesion and emigration into the local tissue is a multistep process started by the tethering of cells to the vessel wall in the vascular shear flow. This is followed by rolling along the wall, by the development of a firm adhesion, and, finally, by diapedesis (*1*). The selectins, a family of three adhesion molecules, support tethering and rolling by rapid association and dissociation with carbohydrate ligands (*2*). All members of the family are transmembrane glycoproteins and share a highly conserved N-terminal Ca^{2+}-dependent (C-type) lectin domain (*3*). These lectin domains preferably recognize oligosaccharide epitopes related to sLex and stereoisomers thereof (*4*) with very low affinities (K_d = 0.1−5 mM) (*5*, *6*). However, it was found that the physiological ligands (a small group of sLex[1]-containing mucin-like glycoproteins) are bound with much higher affinities (≤100 nM) (*7*). Multiple protein−carbohydrate interactions mediated by a specific molecular arrangement of the binding epitopes within the mucins are therefore thought to be the reason for a higher binding efficiency (*8*). Several oligomeric sLex derivatives have been prepared to test this hypothesis, but up to now this approach could only in part support the multivalency hypothesis (*9*, *10*).

Despite these open questions, the dynamics of the selectin−ligand interactions as the basis for the cell rolling process could excellently be illustrated by several in vitro flow chamber studies in recent years. Detailed investigations of the leukocyte rolling under shear flow conditions could demonstrate that tethering and rolling are regulated by the kinetics of bond formation and dissociation, which are

[†] This work was supported by the Deutsche Forschungsgemeinschaft, Sonderforschungsbereich 197/B11, and the Leopoldina Foundation (BMBF 9901/8-6).

* Correspondence should be addressed to this author at the Department of Pharmacy, Martin-Luther-University Halle, Wolfgang-Langenbeck-Strasse 4, D 06120 Halle, Germany. Tel.: 49 345 5525188; Fax: 49 345 5527022; E-mail: bendas@pharmazie.uni-halle.de.

[#] Dedicated to Professor Dr. Peter Nuhn on the occasion of his 65th birthday.

[‡] University of Groningen.

[§] Department of Pharmacy, Martin-Luther-University Halle.

[∥] University Konstanz.

[⊥] Institute of Physiological Chemistry, Martin-Luther-University Halle.

[1] Abbreviations: AFM, atomic force microscopy; CHO-E, Chinese hamster ovarial cells containing E-selectin; DSPC, 1,2-distearoyl-*sn*-glycero-3-phosphocholine; EO, ethoxyethylene/ethylene glycol unit; NBD-PC, 1-palmitoyl-2-[12-[(7-nitro-2,1,3-benzoxadiazol-4-yl)amino]-dodecanoyl]-*sn*-glycero-3-phosphocholine; sLex, Sialyl Lewis X epitope [α-Neu5Ac-(2→3)-β-D-Gal-(1→4)-[α-L-Fuc-(1→3)]-β-D-GlcNAc-(1→R)].

10.1021/bi0117596 CCC: $22.00
Published on Web 02/22/2002

different for each of the individual selectins (*11*−*13*). Furthermore, it was found that force-dependent cell deformation results in a subsequent increase in the number of contact points. For this reason, a dynamic balance between formation and breakage of selectin−ligand bonds is reached over a wide range of wall shear stress and ligand density (*14*).

In a recent study, we combined the dynamic investigation of the selectin-induced cell rolling with exploring the hypothesis of multivalent ligand binding (*15*). For this purpose, we incorporated a naturally occurring sLex−glycosphingolipid (sLexLacCer in Figure 1) into planar support-fixed phospholipid model membranes to simulate the conditions at the cell surface. By using the Langmuir technique, we could modify the concentration and distribution of the glycolipids within the phospholipid matrix to obtain a correlation between lateral ligand organization and cell binding events. These experiments demonstrated that a lateral clustering of the glycolipids appears to be an essential prerequisite for efficient selectin recognition, thus supporting the hypothesis of multivalent ligand−receptor interactions as basis for cell rolling.

In the present study, we focused these dynamic rolling experiments on the molecular features of the glycolipid ligands. Special emphasis was put on the evaluation of the influence of ligand mobility and flexibility on the rolling process. For this purpose, we used a series of sLex-based glycolipids that differed in the spacer structures inserted between the hydrophobic moiety and the terminal sLex. This allowed us to gradually vary headgroup accessibility and flexibility at the membrane surface. We compared glycolipids containing ethylene glycol spacers with those carrying lactose spacer units instead. The latter were similar in size but displayed a restricted mobility. Depending on the molecular structure of the glycolipids and their concentration, differences in their supramolecular organization in the film had to be anticipated. A laterally clustered arrangement of the glycolipids was shown using epifluorescence and atomic force microscopy. In our dynamic flow chamber model, a correlation between ligand flexibility (or mobility) and their ability to mediate rolling could be established. The results of these model experiments support the importance of epitope flexibility on natural mucin-like ligands for cell rolling.

EXPERIMENTAL PROCEDURES

Materials. 1,2-Distearoyl-*sn*-glycero-3-phosphocholine (DSPC) was purchased from Sigma (Deisenhofen, Germany). 1-Palmitoyl-2-[12-[(7-nitro-2,1,3-benzoxadiazol-4-yl)amino]-dodecanoyl]-*sn*-glycero-3-phosphocholine (NBD-PC) was purchased from Avanti Polar Lipids (Alabaster, AL). The sLex-based glycolipids were synthesized as previously published (*16*−*18*). All substances were used without further purification.

Cell Cultivation. E-selectin-transfected CHO cells (CHO-E cells) of mice were grown in MEM-α media containing 10% fetal calf serum, 2 mM L-glutamine, and 100 nM penicillin/streptomycin. Flasks seeded with 5×10^4 CHO-E cells were incubated at 37 °C in 5% CO_2 for 3−4 days to near-confluency. After trypsinization for 3 min with 2 mL of 0.25% trypsin/EDTA, the cell suspension was transferred to slowly rotating plastic tubes. The cells remained in suspension for up to 4 h. Within this time, the rolling experiments were performed in the flow chamber.

Preparation of Supported Planar Bilayers. Supported planar bilayers were prepared using the Langmuir−Blodgett technique. Microscopy slides (glass, diameter of 18 mm, thickness of 0.2 mm) were used as transparent supports. The slides were treated to achieve a highly homogeneous surface as follows: The slides were incubated in a concentrated H_2SO_4/H_2O_2 mixture (7:3) at 80 °C for 30 min under ultrasonic conditions, and were then rinsed with ultrapure water for 30 min. To increase the density of silanole groups at the surface, a cleaning procedure with $NH_3/H_2O_2/H_2O$ (1:1:5) was performed, followed by a final rinse with ultrapure water and drying of the slides. To form a supported bilayer, monochlorodimethyloctadecyl-silane (Sigma, Deisenhofen, Germany) was bound covalently to the surface of the slide at 50 °C for 30 min, resulting in a hydrophobic monolayer. A DSPC film containing the desired concentration of a glycolipid ligand was preformed on the Langmuir trough. The bilayer on the slide was completed by transfer of this X-type monolayer to the hydrophobic substrate at a lateral pressure of 38 mN/m and a speed of 0.5 mm/min. The transfer ratios were between 0.95 and 1. Freshly prepared supported bilayers were immediately used for experiments in the flow chamber.

Film Balance and Fluorescence Film Balance Experiments. The monolayer investigations were carried out on a purpose-built film balance based on a rectangular Teflon trough (area 140 cm^2, 1 cm depth) equipped with a thermostat. The surface pressure was measured using a commercial Wilhelmy balance system (R&K GmbH, Mainz, Germany). For all film balance experiments, the pure glycolipids as well as their mixtures were dissolved in chloroform/methanol 2:1 (v/v) at a concentration of about 1 mM. The lipid solution was spread on the air/water interface with a microsyringe. The self-assembled lipid films were equilibrated to zero surface pressure for 10 min before the experiments were started. Compression was performed at 25 °C with a speed of 0.01 $nm^2\ min^{-1}\ molecule^{-1}$.

All experiments were performed at 25 °C. Borate buffer (pH 7.4) containing 150 mM NaCl, 10^{-4} M Ca^{2+}, and 10^{-4} M Mg^{2+} was favored as sub-phase, as its compatibility with the flow medium in the cell rolling experiments has been confirmed previously.

To allow epifluorescence studies, the film balance was combined with a fluorescence microscope (Olympus Optical Co. GmbH, Germany) and a camera "Proxicam" (Proxitronic KG, Bensheim, Germany). NBD-PC was used as fluorescent dye and added to the lipid mixture at a concentration of 0.5 mol %. This dye does preferentially dissolve in the fluid phase. Quantification of the relative fluorescent area was performed using Biorad Quantity one software v1.1 (BioRad, Munich, Germany), and the number of positive pixels was calculated using a standard. Background levels were selected according to the individual intensity distribution of each image. All experiments were repeated for 4 times.

Laminar Flow Experiments. The parallel plate flow chamber used in these studies has been described in detail in our previous investigations (*19*). The flow apparatus was mounted onto the inverted fluorescent microscope Axiovert 135 of a Laser Scanning Microscope (LSM 410 invert, Carl Zeiss).

Adhesion experiments were performed at 25 °C in a temperature-controlled environment to maintain the lateral

structure of the model membrane. MEM-α was used as flow medium at a shear rate of about 200 s^{-1} driven by hydrostatic pressure. For the flow experiments, 10^6 fluorescently marked CHO-E cells (Calcein AM, Molecular Probes, Leiden, The Netherlands) in 100 μL of medium were injected into the streaming medium without dilution. The flow was stopped for 5 min to allow interaction of the cells with the supported membrane. After this period, shear force was applied, and the adhesion behavior of the cells was monitored by a sequence of images taken every 2 s. To characterize the cell movement, 50−150 cells within an area of 630 × 630 μm were analyzed throughout a 20 s period. Only those cells which adhered to the membrane without contact to other adhered cells were counted and analyzed. The experiments for the presented data were repeated at least 4 times.

Atomic Force Microscopy. AFM measurements were performed on an AFM Nanoscope III dimension 5000 (Digital Instruments, Santa Barbara, CA). The microscope was vibration-damped. Commercially available pyramidal Si_3N_4 tips (NCH-W, Digital Instruments, Santa Barbara, CA) on a cantilever with a length of 125 μm were used. All investigations were carried out in Tapping mode in order to prevent damage to the sample surface. The resonance frequency was approximately 220 kHz, and the nominal force constant was 36 N/m. The scan speed was chosen as a dependence on the scan size while the scan frequency was always between 0.5 and 1.5 Hz. The results were visualized in either height or amplitude mode. All samples were examined within 1 h after preparation at a relative humidity of 60%.

RESULTS AND DISCUSSION

Molecular Features of the Glycolipid Ligands. The naturally occurring selectin ligands are mucin-like glycoproteins, which display the carbohydrate binding epitopes as side chains on a highly flexible protein backbone. The importance of this flexibility for mediating tethering and rolling of cells in the shear flow has often been postulated, but never been proven in model experiments.

Few studies report on glycolipids as selectin ligands. SLex-based ceramides have been isolated from granulocytes (*20*, *21*), and their selectin binding ability could be demonstrated in flow chamber experiments (*22*). In a previous study, we embedded a synthetic but naturally occurring sLex-ceramide into various phospholipid matrixes and showed that these glycolipids can act as rolling ligands when they are arranged in lateral clusters (*15*). This glycolipid contained a lactose spacer between the ceramide anchor and the sLex headgroup, which resulted in lower accessibility and flexibility than in the natural sialomucins.

Continuing these experiments, we further investigated the influence of the headgroup flexibility at the membrane surface on cell rolling. We introduced synthetic neoglycolipids, which differ in their spacer structures between the sLex headgroup and the membrane anchor. A 1,2-di-*O*-hexadecyl-*sn*-glycerol was used as hydrophobic moiety in all cases. During one procedure, segments of three EO units, which mimic the length of a naturally occurring lactose or lactosamine spacer, were inserted stepwise to obtain the sLex derivatives. The sLex lipid without spacer (sLex0) has not been discovered to occur in nature. The compounds with either 3, 6, or 9 EO unit spacers (sLexEO3, sLexEO6, sLexEO9) correspond to the naturally occurring sLex, dimer sLex, or trimer sLex glycosphingolipids (*17*). In another procedure, lactose segments were introduced as spacers (*18*). The resulting compounds containing either 1, 2, or 3 lactose units (sLexLac1, sLexLac2, or sLexLac3) had spacer length comparable to the EO-spacered glycolipids (Figure 1), but instead displayed a lower degree of molecular flexibility, as demonstrated by NMR investigations (publication in preparation). To confirm the size dimensions, molecular modeling calculations were performed, which revealed that three EO units have a length of about 0.93 nm in the all-trans conformation, comparable to one lactose unit of 0.88 nm (examples for sLexEO3 and sLexLac1 in Figure 2). Under this assumption, the spacer length of the compounds sLexEO3, sLexEO6, and sLexEO9 should be comparable to sLexLac1, sLexLac2, and sLexLac3. Differences in the cell rolling characteristics on model membranes containing these structurally homologeous glycolipids should therefore reflect the influence and importance of ligand mobility and epitope flexibility. The natural analogue sLex ceramide (*16*, *18*), which was used in our previous investigations, was applied as internal control.

Characterization of the Model Membranes by Π/A Isotherms. To find a correlation between cell rolling characteristics and lateral ligand distribution, the resulting model membranes were thoroughly analyzed by physicochemical means. The supramolecular organization of the ligand is generally determined by the molecular structure and the intermolecular interaction phenomena including van der Waals interactions, electrostatic dispersion forces, sterical disorder, hydrogen bonds, and hydration. In addition, mixing of the glycolipids into the matrix lipid DSPC will cause further interactions between the components, which might influence the lateral lipid distribution.

Continuous Π/*A* isotherms of both the pure lipid systems and their mixtures with DSPC were recorded at 25 °C (Figure 3). The natural sLex ceramide film was in a liquid-condensed state, since no first-order phase transition nor major changes in the compressibility could be observed. The synthetic glycolipid without spacer sLex0 showed a slightly different compression behavior. The lift-off area was shifted to a larger value, and the compressibility was generally increased. In addition, the compressibility of the film changed between 10 and 20 mN/m. We conclude that the molecular organization within the film was different below and above this region. This may be described as a not well-defined phase transition.

Pure Glycolipid Films. The insertion of 3 and 6 EO units into the glycolipid (sLexEO3, sLexEO6) induced a first-order phase transition at pressures between 27.4 and 35.0 mN/m. Below the phase transition, the films of both glycolipids were more fluid and compressible. The lift-off area increased with spacer length. The collapse pressure increased as well, but the corresponding molecular area was almost unchanged (Table 1). This indicates that, in the condensed state, the molecular area is determined by the size of the headgroup. The latter was calculated as 0.52 nm^2, whereas the two alkyl chains only require approximately 0.4 nm^2 (Figure 2). In conclusion, the molecular area in the condensed state is obviously determined by the carbohydrate headgroup, whereas the crystallization is apparently controlled by hydrophobic

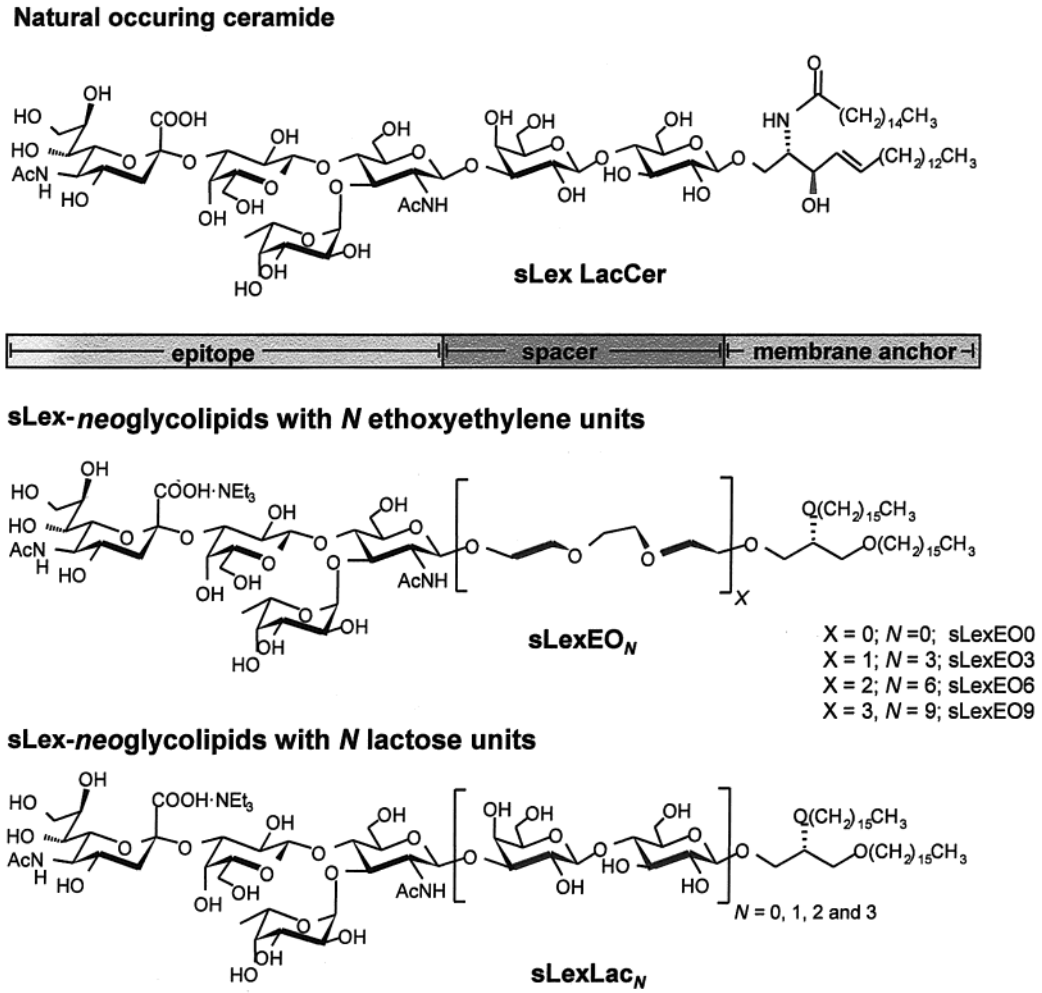

FIGURE 1: Structures of the natural sLex-ceramide and the synthetic sLex-neoglycolipids with different ethoxyethylene or lactose spacers and a schematic comparison of their sizes.

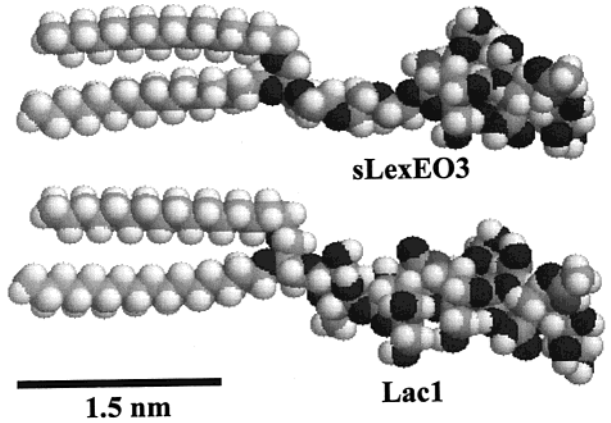

FIGURE 2: Space-filling models of the synthetic sLex-neoglycolipids sLexEO3 (top) and sLexLac1 (bottom). The models were calculated with Alchemy.

and van der Waals interaction between the hydrocarbon chains.

The film of the glycolipid with the longest EO spacer, sLexEO9, showed a different phase behavior. The very compressible monolayer was in a permanent liquid-expanded state. Surprisingly, the collapse pressure was found to be as low as 30 mN/m (A_c = 0.93 nm^2). The organization of the glycolipids in the fluid, liquid-expanded state will depend on the flexibility, the electrostatic repulsion, and the hydration of their headgroups. It is known from EO-spacered alkanes that an increasing number of EO units causes a fluidization of the film (*23*). This is reflected in a widening of the collapse areas and a shift of the first-order transition to higher pressures. The longer the spacer, the larger the water shell surrounding the headgroup. At low pressures, the EO units are organized in random coils and not oriented perpendicularly within the membrane. In contrast, a more ordered organization may be favored by molecules with a short spacer or at higher pressures. Under these conditions, the spacers are in a stretched-out formation, and the headgroups are displayed on the surface. On the other hand, the longer EO-spacers are more flexible, and no attractive interaction forces do exist. The only behavior exhibited by molecules with longer EO-spacers was repellence at the water shell and entropic disordering. As illustrated in Figure 4, the accessibility of the carbohydrate terminus might decrease from sLexEO3 and sLexEO6 to sLexEO9.

In a second set of experiments, the glycolipids with lactose spacers were analyzed. Under the assumption of similar spacer length, the compounds sLexEO3, sLexEO6, and sLexEO9 should be comparable to sLexLac1, sLexLac2, and sLexLac3. The isotherms of sLexLac1 showed a first-order phase transition at 22.4 mN/m, which was slightly lower than that of the corresponding sLexEO3. The sLexLac1 film was more condensed, which was further confirmed by the smaller lift-off area. The collapse area was only slightly increased

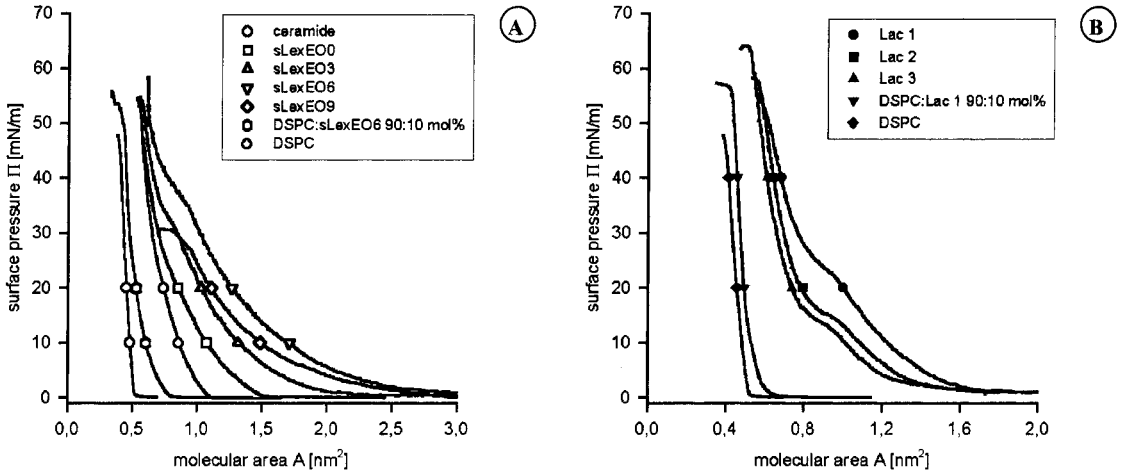

FIGURE 3: Π/*A* isotherms of the investigated pure glycolipid films and their mixtures with DSPC. (A) EO-spacered lipids, (B) lactose-spacered lipids.

Table 1: Characteristic Values of the Collapse Pressure Π_c, the Mean Molecular Area A_c, the Lift-Off A_0 Area, the Transition Pressure Π_t, and the Area A_t for All Glycolipids

lipid	A_0 (nm²)	A_c (nm²)	Π_c (mN/m)	A_t (nm²)	Π_t (mN/m)
sLexLac1	1.60	0.64	53.6	1.12	22.4
sLexLac2	1.40	0.62	57.4	1.11	15.2
sLexLac3	1.34	0.57	60.8	0.92	11.7
sLex0	1.47	0.56	53.0	1.08	10.1
sLexEO3	2.15	0.58	53.4	1.02	27.3
sLexEO6	2.93	0.62	58.0	1.01	35.0
sLexEO9	2.75	0.93	30.0	–	–
sLexLacCer	1.09	0.55	52.0	–	–
DSPC	0.51	0.41	44.3	–	–

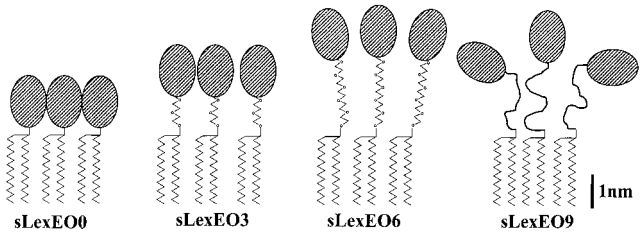

FIGURE 4: Suggested model of the molecular organization of the EO-spacered glycolipids in a membrane representing the correct intramolecular size relations.

($\Pi = 53.6$ mN/m, $A = 0.64$ nm²). However, sLexLac2 and sLexLac3 showed a decrease in phase transition and an increase in collapse pressure. This indicates that the interaction between their lactose moieties was stronger than the interaction between the EO spacers. In other words, the compressibility of the films decreased, whereas the tendency to form an ordered liquid-condensed state increased. Consequently, the lactose derivatives displayed a lower molecular flexibility and stronger intermolecular stiffness compared to the EO-spacered compounds.

The matrix lipid DSPC itself exhibited a liquid-condensed film behavior during compression. DSPC films are generally very incompressible and collapse at a molecular area of 0.41 nm² and a pressure of 44.3 mN/m. A more detailed description of all systems will be published elsewhere.

DSPC/Glycolipid Mixed Films. To perform cell rolling experiments, the above glycolipids had to be inserted as ligands into a DSPC matrix. For this reason, we also examined the phase behavior of the mixed films. The mixing behavior was dependent on the molecular structure, the concentration, and the lateral pressure of the glycolipids. Typical mixed isotherms are shown in Figure 3. An improved film stability (expressed by an increased collapse pressure) was observed for all mixed films with glycolipid concentrations below 50 mol %. The average molecular area increased to higher values compared to the pure DSPC matrix. Because of the biological background of our investigation, glycolipid concentrations within the matrix lipid should only be varied between 0 and 10 mol %. In this concentration range, deviations in the compression behavior were marginal, whereas the film morphology and the lateral ligand distribution within the model membranes were dramatically different.

Morphological Characterization of the Films. These differences in morphology and lateral distribution were visualized by epifluorescence microscopy (Figure 5) and, with higher resolution, by AFM (Figure 6).

The plain matrix lipid DSPC displayed a fluorescence image that is typical for a condensed film with large aggregated and irregular shaped dark domains, when examined at pressures above the lift-off (data not shown).

Pure Glycolipid Films. The typical appearance of a fluid film with an evenly distributed fluorescent dye could be observed for all glycolipids below the phase transition, as well as for sLexEO9 over the whole pressure range (Figure 5A). At the onset of the phase transition, small dark round-shaped domains became visible. Their size and shape were dependent on the molecular structure and differed among the glycolipids. The EO-spacered sLex lipids (sLex0, sLexEO3, sLexEO6) showed very small domains between 1 and 2 μm. As an example, the organization of sLexEO3 at 25 mN/m is shown in Figure 5B. The size of the domains expanded with increasing lateral pressure. In the collapse region (about 50 mN/m), almost 70% of the total surface consisted of condensed domains with a maximum size of 5 μm.

In the case of the lactose-spacered lipids, the domain size was larger at comparable lateral pressures. Here, the domains grew fast after reaching the phase transition pressure from 1 μm to values of about 10 μm (Figure 5C). More than 80% of the surface consisted of condensed domains at the collapse pressure (53 mN/m). The higher condensation tendency supports the assumption that the molecular interactions

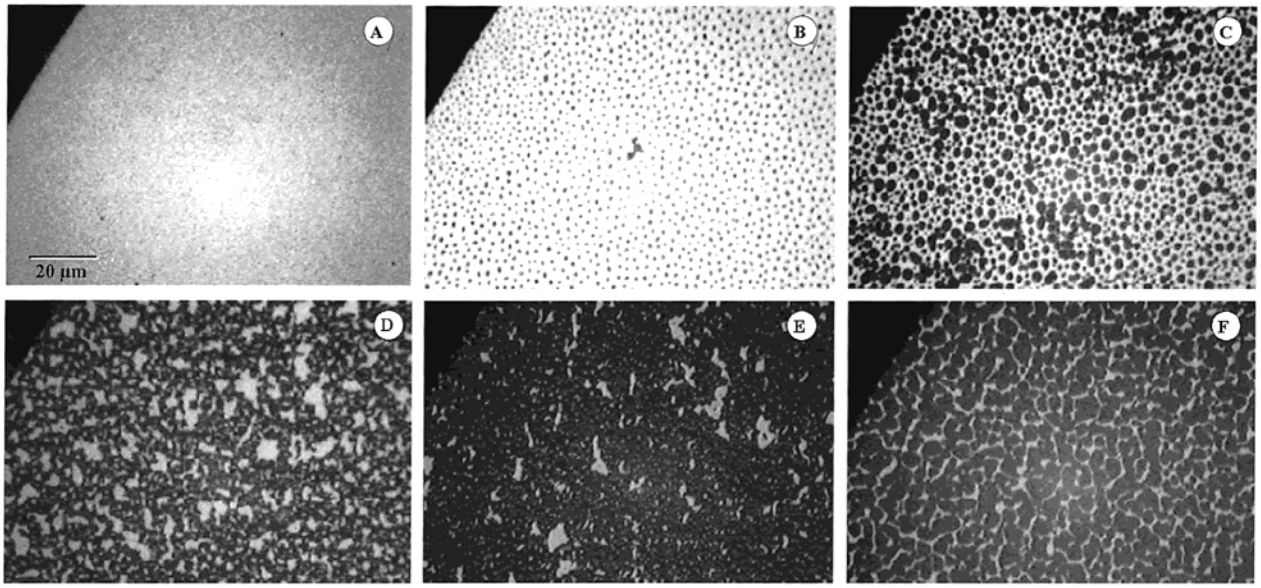

FIGURE 5: Typical fluorescence micrographs of pure and mixed model membranes consisting of (A) sLexEO9, (B) sLexEO3, (C) sLexLac1, (D) DSPC/sLexEO6, 90:10 mol %, (E) DSPC/sLexEO6, 95:5 mol %, and (F) DSPC/sLexLac2, 90:10 mol %. All images were recorded at a surface pressure of 25 mN/m (25 °C).

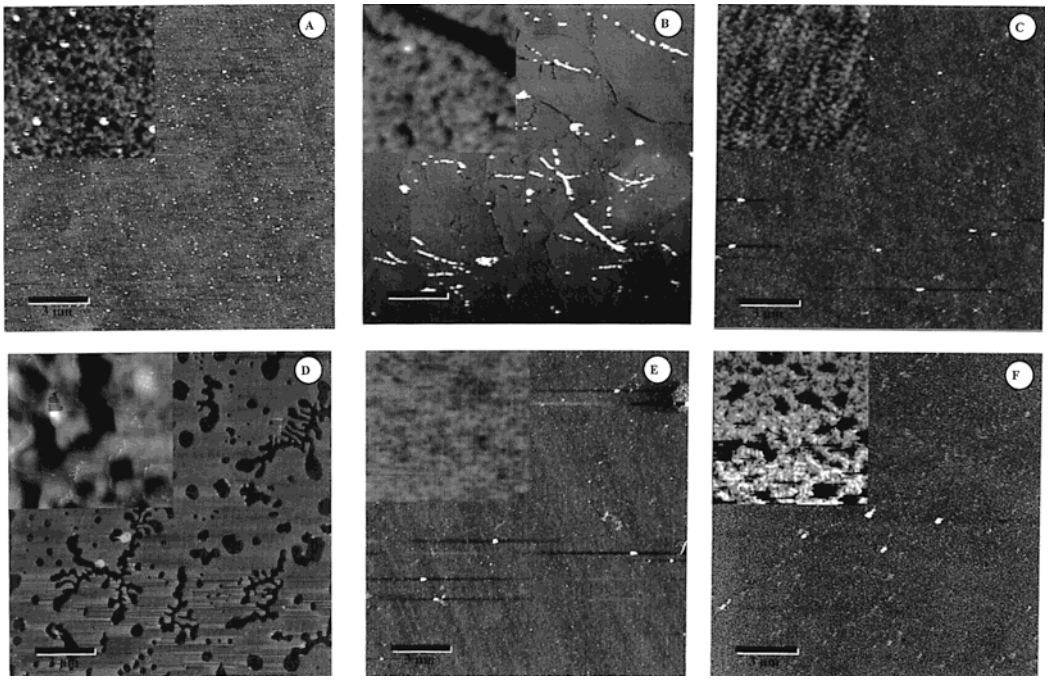

FIGURE 6: Typical AFM images of the model membranes used in this study. (A) sLexEO6 with smooth surface and small round glycolipid clusters of approximately 20 nm (amorphous structure); (B) sLexLac1 surface is dominated by hexagonal domains of 5−10 μm in size; (C) sLexLac2 forms a homogeneous film; the insert demonstrates small well-ordered clusters of 20 nm in size; (D) DSPC/sLexEO6, 90:10 mol %; dark areas representing phase-separated glycolipids surrounded by condensed DSPC; the fluid areas vary in size between 200 nm and 1 μm; (E) DSPC/sLex0, 90:10 mol %; appears as homogeneous film with only very small cluster-like irregularities; (F) DSPC/sLexLac2, 90:10 mol %; appears as a smooth surface film containing crystalline substructures and fractal clusters. (Bar represents 3 μm in all images; insert size 600 × 600 nm, transfer pressure 30 mN/m at 25 °C.)

between the lactose-spacered molecules are stronger than in the case of the EO-lipids.

The supported glycolipid films were also investigated by AFM to obtain further insight into their lateral structure and morphology. Typical lateral organizations of the pure glycolipid films are shown in Figure 6A−C. The morphology of the glycolipid clusters was strictly dependent on their tendency to associate. The sLexEO6 film was representative for the condensed film structure of all EO-spacered glycolipids and is shown in Figure 6A. In the overview, the surface appeares smooth without any breaks. The heighth difference between lower and upper areas was only 0.75 nm at a total thickness of the film of 4.2 nm. At higher resolution, it could be observed that the condensed phase was not highly ordered and no defined crystal lattice was formed. Within these domains, the glycolipids were organized in ordered and tightly packed clusters of 20 nm in size (insert in Figure 6B). It could be estimated that each of these clusters contained about 200 glycolipid molecules. The amorphous appearance of these films might be the result of the size

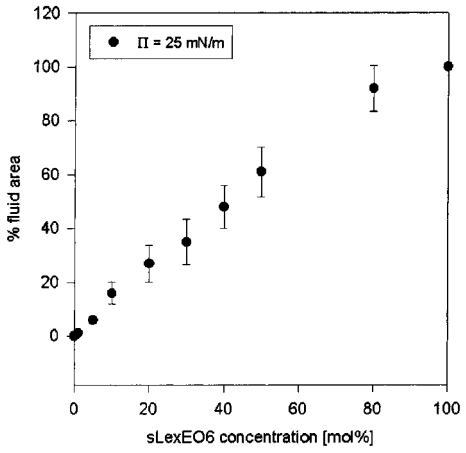

FIGURE 7: Correlation between the total fluid area and the glycolipid concentration within the model membrane. The fluid area was calculated from a densitometric analysis of the epifluorescence images.

differences between the large headgroup and the relatively small tail. This can force the molecule into either a tilted position within a homogeneous area or smaller round clusters. It can be concluded that the van der Waals interactions between the hydrophobic tails are not able to dominate the system at increasing headgroup/spacer size and well-defined crystals cannot form.

In case of the lactose-spacered lipids, two morphological assemblies could be visualized (Figure 6B,C). The lipid sLexLac1 formed hexagonally shaped condensed domains with sizes between 1 and 5 μm above the phase transition. Within these domains, the glycolipids were organized in ordered and tightly packed clusters of 20 nm in size. It can be expected that the lipid sLexLac2 with a lower phase transition than sLexLac1 should have a higher association and condensation tendency. In fact, no domain formation could be observed after film transfer. A homogeneous and well-ordered film consisting of small clusters of 10−20 nm in size was formed. The clusters created homogeneously organized superstructures within the films, but a crystalline network could not be found. The morphology of the longest lactose lipid sLexLac3 was comparable to sLexLac2 with a tendency to form even more ordered films.

DSPC/Glycolipid Mixed Films. The mixing of a fluid glycolipid with a condensed matrix lipid typically results in phase-separated films. Epifluorescence microscopy showed that the fluid, brightly fluorescent areas were surrounded by a dark DSPC matrix (Figure 5D−F). This confirmed that all glycolipids were phase-separated and can be regarded as locally clustered. The shape and the size of the glycolipid clusters varied substantially depending on the nature of the lipids and its concentration within the film. Irregular fractal fluid domains were typical for a film of 10% sLexEO6 in DSPC (Figure 5D). To detect the influence of reduced glycolipid concentrations on clustering, we also investigated films containing 5−0.1 mol % of sLexEO6. A reduction in glycolipid concentrations reduced the number of clusters and also their size as illustrated in Figure 5E (5 mol % sLexEO6). The relative total area occupied by the glycolipid clusters dependent on the glycolipid concentration was determined by densitometry. The diagram given in Figure 7 shows the linear correlation between the glycolipid concentration and the fluid area. This suggest that the demixed glycolipid cluster may also be present at very low concentrations that are potentially below the detection limit.

The mixed films containing sLexLac-glycolipids had smaller fluorescent areas than DSPC/sLexEO films at the same concentrations. This can be attributed to stronger interactions between the lactose-spacered lipids (Figure 5F).

The laterally phase-separated films of all glycolipids within the rigid DSPC matrix were also investigated by AFM. A typical film of DSPC containing the fluid sLexEO6 (90:10 mol %) is shown in Figure 6D. Round-shaped and fractally structured domains of the glycolipid were homogeneously distributed all over the film. The size of these domains varied between 100 nm and 1 μm. In contrast, the mixture of sLex0 and DSPC showed a smooth surface morphology without any visible substructures (Figure 6E) in a wide range of glycolipid concentrations (0.1−10 mol %). The film behavior implies either a molecular miscibility or a homogeneous distribution of very small aggregates of only a few molecules.

The sLexLac lipids (Figure 6F) had a strong tendency to form highly condensed surface structures, which is in full agreement with the fluorescence investigations (Figure 5F). As discussed above, this may result from strong intermolecular interactions either among the sLexLac lipids or within the matrix lipid.

The observations confirm cluster formation of all spacered glycolipids within the DSPC matrix. This will have to be considered in the interpretation of the cell rolling experiments. The higher tendency of the sLexLac lipids to form condensed clusters compared to the EO-spacered glycolipids may be attributed to stronger intermolecular forces among the lactose spacers and leads to gradual differences in the mobility and flexibility of the sLex headgroups at the surface of the model membranes.

Cell Rolling Investigations. To investigate the capacity of the sLex-glycolipids to mediate selectin-induced cell rolling, the previously described dynamic model system was employed (*15*). Using the Langmuir−Blodgett technique, DSPC model membranes containing a defined concentration of a glycolipid ligand were prepared and subsequently transferred to a coverglass used as solid support. After mounting of the glass into a flow chamber, fluorescently labeled Chinese hamster ovarial cells that exhibit stable amounts of E-selectin (CHO-E) were allowed to interact with the model membrane under static conditions for 5 min. Then, cell adhesion and rolling at a shear rate of 200 s^{-1} were observed by fluorescence microscopy.

Our previous investigations demonstrated that, in contrast to the common static binding assays which solely focus on cell adhesion at high ligand concentrations, very low densities of glycolipid ligands are sufficient to mediate rolling—a process sensitively balanced between firm adhesion at higher concentrations and detachment at lower concentrations.

Initially, we introduced EO-spacered compounds. At glycolipid concentrations between 10% and 0.1%, no cells within the analyzed area showed any motion. Further reduction of the ligand density resulted in strong differences in the behavior of the different ligands (Figure 8a). The spacerless glycolipid sLex0 was not able to mediate adhesion and rolling below 0.1%, and all cells were detached immediately. This might be attributed to the restricted accessibility of the headgroup at the DSPC membrane surface. Furthermore, this glycolipid displayed no phase borders in

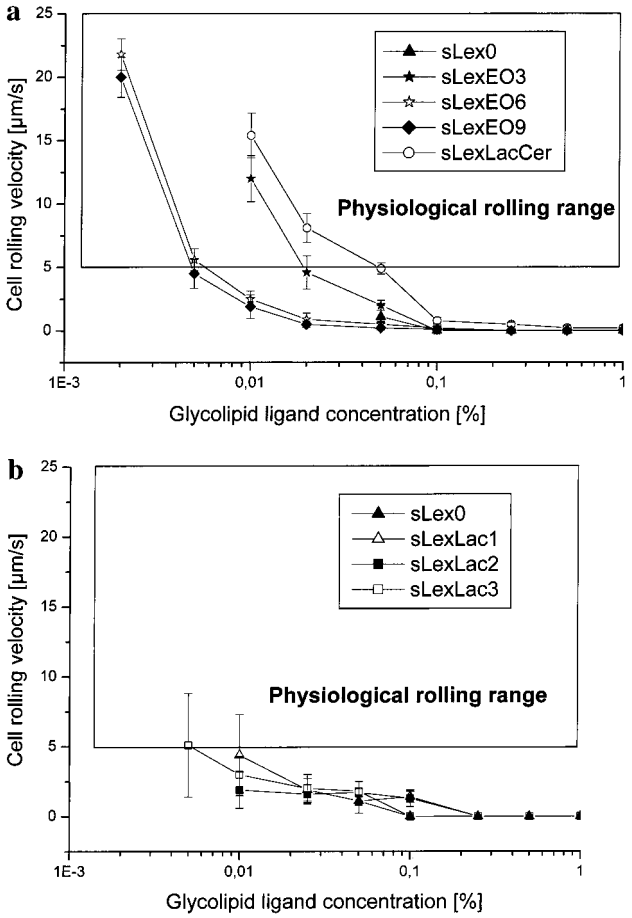

FIGURE 8: Cell rolling velocity of CHO-E cells along model membranes containing varying concentrations of the indicated glycolipid ligands at a shear rate of 200 s^{-1}. (a) Membranes with EO-spacered glycolipids in comparison to the naturally occurring ceramide; (b) sLexLac-containing membranes.

the AFM images (Figure 6E) and may therefore be distributed within the DSPC matrix. Lateral ligand clustering is an essential prerequisite for rolling, as we showed in previous experiments.

The other EO-spacered glycolipids that could be shown to cluster in the DSPC matrix (see Figures 5D,E and 6D) mediated a jerky motion of the cells at a velocity between 5 and 20 μm/s along the membrane (versus 1−2 mm/s of the free flowing cells). This can be regarded as cell rolling (Figure 8a). We conclude that spacer elongation, which corresponds to an increase in headgroup flexibility, is of crucial importance for cell rolling. While sLexEO3, containing a three EO-unit spacer, required at least a concentration of 0.01% to mediate rolling at a velocity between 5 and 12 μm/s, the longer spacered sLexEO6 and sLexEO9 were more effective ligands with detectable activity at concentrations of 0.005−0.001%. Additionally, sLexEO6 and sLexEO9 mediate rolling at a higher velocity than sLexEO3. The percentage of rolling cells was between 60 and 80% in each case, relative to the number of cells that adhered initially under static conditions. These results reflect a correlation between spacer length, headgroup flexibility, and the ability to mediate rolling.

To confirm this finding, we investigated the lactose-spacered derivatives sLexLac1, -2, and -3, which differed only in the stiffness of their spacer compared to the EO-glycolipids. However, these compounds displayed a completely different behavior than the EO-spacered sLex-lipids (Figure 8b). At concentrations below 0.1%, they did mediate only a very slow cell movement of up to 5 μm/s, which cannot be regarded as true cell rolling. Despite increasing spacer length, there were almost no differences among these compounds. Only a change in ligand concentration did influence the activity of the glycolipid membranes. All cells detached from the membrane when less than 0.01% of sLexLac1 or sLexLac2 was used, while 0.005% of the longest derivative sLexLac3 was sufficient. These results indicate that there must other factors that are important for cell rolling in addition to spacer length and headgroup accessibility: (i) the intramolecular flexibility of the ligands themselves, and (ii) molecular mobility caused by supramolecular interactions between the clustered molecules.

This hypothesis is supported by the different appearance of both EO and Lac lipids in the AFM images. Since the sLexLac lipids displayed more rigid, highly structured clusters in the DSPC matrix (indicating restricted molecular mobility and flexibility), they are unable to act as effective ligands.

A comparison of the behavior of sLexLac1 and the ceramide glycolipid appears conflicting, since both glycolipids differ only in the hydrophobic moiety. Whereas the ceramide is well suited to mediate rolling, the dihexadecyl glycerol-anchored sLexLac1 was not. This suggests that also the membrane anchor does play an active role in ligand presentation. This can in part be explained by differences in the intermolecular interactions among ceramides and dialkyl glycerols. Furthermore, due to its amide, the ceramide has a larger interfacial area compared to the glycerol backbone. A larger molecular area allows better headgroup hydration, which might also cause a higher molecular mobility within the glycolipid-rich domains. Consequently, despite differences in the spacer structures, the ceramide is much more comparable to sLexEO3 with respect to flexibility and spacer length. However, these studies are an initial approach to understand the mechanical requirements of rolling ligands, which might give an insight into the way natural selectin ligands work.

Only few studies consider the mechanical properties of selectins and their ligands and the implications for rolling under in vitro conditions, but the naturally occurring mucin-like glycoproteins could barely be modified systematically to get a clear correlation between structural and functional properties. Puri et al. reported on the chemical modification of the L-selectin ligand CD34, which can change its mechanical properties (*24*). The periodate-oxidized glycoproteins displayed a higher resistance to detachment and slower rolling velocities. Since this modification has no influence on the binding affinity in the absence of shear, this effect was attributed to changes in the elasticity and spring constants in the mucin-like region, which indirectly underscores the importance of ligand flexibility for rolling. Other experiments demonstrated the importance of the extended length of the selectin receptors for rolling. Patel et al. investigated neutrophil rolling on P-selectin, which was gradually deleted with its consensus repeats (*25*). A minimal number of five consensus repeats was necessary to give P-selectin the sufficient length and flexibility to allow neutrophil rolling.

In contrast, the stepwise structural modification of the artificial rolling ligands in our experiments offers for the first time a clear correlation between peculiarities of the ligand structure such as intramolecular flexibility or restricted intermolecular mobility, and the ability to mediate rolling. The proper presentation of the binding epitopes depends both on their accessibility at the membrane surface (largely influenced by the length and flexibility of the introduced spacers) and, perhaps even more important, on the freedom of molecular movement within the clustered ligand-rich assemblies.

CONCLUSIONS

Over the last years, the molecular mechanisms of selectin-induced leukocyte rolling along the endothelial surface have been increasingly understood as a highly regulated process, which represents a dynamic balance between formation and breakage of selectin−ligand bonds over a wide range of external parameters. A series of dynamic in vitro studies demonstrated that the kinetics of bond formation and dissociation of selectins are the basis for rolling, regulated and controlled by factors such as wall shear stress, ligand density, or cell deformation. These studies, which in most cases used isolated selectins or natural selectin ligands, mainly focused on the kinetic aspects of the receptor−ligand interactions. Using the natural compounds, which could not be modulated in their structural characteristics, a correlation between the physical properties of the ligands including flexibility, molecular shape, or length and their ability to mediate cell rolling was impossible to establish so far. Therefore, we performed this in vitro cell rolling study on a series of seven sLex-based neoglycolipids as artificial ligands. The glycolipids used in this study differed only in their spacer structures placed between the membrane anchor and the sLex binding epitope. These molecules are therefore excellently suited to examine the influence of headgroup mobility on the ability to mediate cell rolling.

Our approach was to incorporate the glycolipid ligands into support-fixed model membranes to simulate the endothelial surface. The selectin-induced cell rolling could be demonstrated to be strongly dependent on the lateral ligand distribution within these model membranes. Lateral clusters, appearing as multivalent binding epitopes, are an essential prerequisite for rolling. Consequently, we first analyzed the mixing behavior of the glycolipids in the DSPC matrix by fluorescence microscopy and AFM. A lateral separation of the glycolipids and formation of ligand clusters were observed.

The rolling investigations could prove that a minimal accessibility of the headgroup epitope at the membrane surface is required and an increased headgroup mobility can enhance the ability of the ligands to mediate rolling. The absolute length of a spacer is of less importance than flexibility, which results from the intramolecular flexibility of the glycolipids itself and from the intermolecular interactions within the supramolecular associates. Considering these findings, it appears that the extended and highly flexible mucin structure is the ideal substrate for cell rolling under shear force conditions.

ACKNOWLEDGMENT

We thank Ursula Goder for excellent technical assistance and Professor Gösele (MPI für Mikrostrukturphysik, Halle) for supporting the AFM measurements. Dr. Carsten Kneuer is gratefully acknowledged for the fluorescence measurements.

REFERENCES

1. Springer, T. A. (1995) *Annu. Rev. Physiol. 57*, 827−872.
2. Tedder, T. F., Steeber, D. A., Chen, A., and Engel, P. (1995) *FASEB J. 9*, 866−873.
3. Vestweber, D., and Blanks, J. E. (1999) *Physiol. Rev. 79*, 181−213.
4. Phillips, M. L., Nudelman, E., Gaeta, F. C. A., Perez, M., Singhal, A. K., Hakomori, S., and Paulson, J. C. (1990) *Science 250*, 1130−1132.
5. Jacob, G. C., Kirmaier, C., Abbas, S. Z., Howard, S. C., Steininger, C. N., Welply, J. K., and Scudder, P. (1995) *Biochemistry 34*, 1210−1217.
6. Cooke, R. M., Hale, R. S., Lister, S. G., Shah, G., and Weir, M. P (1994) *Biochemistry 33*, 10591−10596.
7. Ushiyama, S., Laue, T. M., Moore, K. L., Erickson, H. P., and McEver, R. P. (1993) *J. Biol. Chem. 268*, 15229−15237.
8. Welply, J. K., Abbas, S. Z., Scutter, P., Keene, J. L., Broschat, K., Casnocha, S., Gorka, C., Steininger, C., Howart, S. C., Schmuke, J. J., Graneto, M., Rotsaert, J. M., Manger, I. D., and Jacob, G. S. (1994) *Glycobiology 4*, 259−265.
9. Maaheimo, H., Renkonen, R., Turunen, J. P., Penttilä, L., and Renkonen, O. (1995) *Eur. J. Biochem. 234*, 616−625.
10. Kretzschmar, G., Sprengard, U., Kunz, H., Bartnik, E., Schmidt, W., Toepfer, A., Hörsch, B., Krause, M., and Seiffge, D. (1995) *Tetrahedron 51*, 13015−13030.
11. Alon, R., Hammer, D. A., and Springer, T. A. (1995) *Nature 374*, 539−542.
12. Puri, K. D., Finger, E. B., and Springer, T. A. (1997) *J. Immunol. 158*, 405−413.
13. Nicholson, M. W., Barclay, A. N., Singer, M. S., Rosen, S. D., and van der Merwe, P. A. (1998) *J. Biol. Chem. 273*, 763−770.
14. Chen, S., and Springer, T. A. (1999) *J. Cell Biol. 144*, 185−200.
15. Vogel, J., Bendas, G., Bakowsky, U., Hummel, G., Schmidt, R. R., Kettmann, U., and Rothe, U. (1998) *Biochim. Biophys. Acta 1372*, 205−215.
16. Hummel, G. (1998) Ph.D. Thesis, University Konstanz, Faculty of Chemistry.
17. Gege, C., Vogel, J., Bendas, G., Rothe, U., and Schmidt, R. R. (2000) *Chem. Eur. J. 6*, 111−122.
18. Gege, C. (2001) Ph.D. Thesis, University Konstanz, Faculty of Chemistry.
19. Bendas, G., Vogel, J., Bakowsky, U., Krause, A., Müller, J., and Rothe, U. (1997) *Biochim. Biophys. Acta 1325*, 297−308.
20. Stroud, M. R., Handa, K., Salyan, M. E. K., Ito, K., Levery, S. B., Hakomori, S., Reinhold, B. B., and Reinhold, V. N. (1996) *Biochemistry 35*, 758−769.
21. Müthing, J. R., Spanbroek, R., Peter-Katalinic, J., Hanisch, F., Hanski, C., Hasegawa, A., Unland, F., Lehmann, J., Tschesche, H., and Egge, H. (1996) *Glycobiology 6*, 147−156.
22. Alon, R., Feizi, T., Yuen, C. T., Fuhlbrigge, R. C., and Springer, T. A. (1995) *J. Immunol. 154*, 5356−5366.
23. Bakowsky, U., Rettig, W., Bendas, G., Vogel, J., Bakowsky, H., Harnagea, C., and Rothe, U. (2000) *Phys. Chem. Chem. Phys. 2*, 4609−4614.
24. Puri, K. D., Chen, S., and Springer, T. A. (1998) *Nature 392*, 930−933.
25. Patel, K. D., Nollert, M. U., and McEver, R. P. (1995) *J. Cell Biol. 131*, 1893−1902.

BI0117596